FAST ANALYSIS OF CYLINDRICAL WAVEGUIDE DISCONTINUITIES BASED ON A CLOSED FORM GENERALIZED SCATTERING MATRIX MODE MATCHING TECHNIQUE

Anastasios P. Orfanidis*, George A. Kyriacou* and John N. Sahalos**
* Department of Electrical & Computer Engineering, Demokritos University of Thrace, GR-67100, Xanthi, Greece.
** Department of Physics, Aristotle University of Thessaloniki, GR-54066, Thessaloniki, Greece.
E-mail:sahalos@ccf.auth.gr

Abstract

A mode matching scheme for the analysis of concentric cylindrical waveguide step discontinuities is proposed. An analytical evaluation of the involved coupling integrals is performed which results in a very fast and accurate method. The formulation is theoretically verified for the special case of a dominant mode excitation, while different excitations are numerically verified. The results obtained from the analysis of various structures are in a very good agreement with measurements and results given by other investigators. The speed and accuracy of the proposed method make it appropriate to be included within microwave network synthesis algorithms.

1. INTRODUCTION

The analysis and design of corrugated waveguides and corrugated horn antennas as well as components based on them can be reduced to the analysis of waveguide discontinuities. Namely, waveguide discontinuities can be combined in tandem or in parallel for the design of components such as filters, polarizers, phase shifters, impedance transformers and corrugated horn antennas. The Mode Matching technique has been proved to be an efficient and robust technique for the analysis of multiple discontinuities. Moreover, a fast and accurate method implementing the Mode Matching is of primary importance in the development of a microwave network synthesis computer aided design (CAD) tool [1]. The best way to achieve this task is the analytical evaluation of the quantities involved in the analysis rather than the performance of any numerical integration. It is towards this aim that the present work tries to contribute.

For the application of the mode matching technique the boundary conditions at the junction are imposed resulting into integrals, known as coupling integrals. Their numerical evaluation is a very time consuming procedure, while they can be calculated analytically only for simple aperture geometries, as for example the rectangular cross-section. The junction of two cylindrical waveguides was studied

analytically in [2], where closed form expressions for the coupling integrals were given, but only for the special case of a dominant mode (TE_{11}) incidence. In this case only the TE_{1n} and TM_{1n} modes are excited. Recently, the rectangular to circular waveguide junction for the concentric and offset cases were studied analytically. In [3,4] the rectangular waveguide modal functions were expanded into Bessel-Fourier series and matched their coefficients with the corresponding ones of the circular waveguide. For this purpose they transformed the cylindrical coordinate system into a cartesian one at the junction. The resulting coupling integrals, after the transformation, are reduced to known Bessel integrals [5].

Examining the technique employed in [3] it is realized that the key point for the analytical evaluation of the coupling integrals is the coordinate transformation from cylindrical to cartesian system. In this work we applied the above technique to the generalized analysis of an arbitrary incidence mode or multimode excitation of the junction of two circular waveguides. The procedure results to closed form expressions for the generalized scattering matrix of the junction. For this purpose all the coupling integrals are evaluated analytically and thus the required computation time is minimized. Furthermore, since the coupling coefficients are calculated very fast we are now able to include any large number of modes (truncation at a higher number of modes) as required to achieve the desired accuracy, with negligible increase in computation time.

2. FORMULATION

The junction of two circular waveguides with different cross section is considered, as shown in figure 1. A common axis of symmetry (axis-z) is assumed for the two waveguides and their walls are taken as perfect conductors. The electromagnetic field inside each waveguide is expanded into a modal series, e.g. Collin [8, p. 354], and the components transverse to the propagation axis-z are expressed as:

$$\begin{bmatrix} \overline{E}_t \\ \overline{H}_t \end{bmatrix}(\rho,\varphi,z) = \sum_{p=1}^{\infty} \left[F_p e^{-\gamma_p z} \pm B_p e^{\gamma_p z} \right] \begin{bmatrix} \overline{e}_p(\rho,\varphi)/\sqrt{Y_p} \\ \overline{h}_p(\rho,\varphi)\sqrt{Y_p} \end{bmatrix} \tag{1}$$

F_p and B_p are unknown mode coefficients for the pth mode and γ_p is their propagation constant. The subscript p denotes the order of the excited mode numbered in an increasing sequence as they occurred. For example p=1,2,3,.. denotes the modes TE_{11},

TM_{01}, TE_{21}, ...

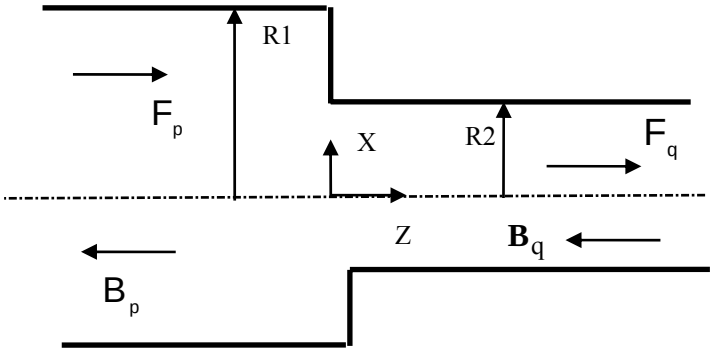

Figure 1. A cylindrical waveguide step discontinuity.

The pth. mode wave admittance Y_p is included in both field expressions for symmetry reasons following Bird [9, 10 p.35] and is given as:

$$Y_p = \begin{cases} y\gamma_p/k & \text{for} \quad TE-\text{modes} \\ yk/\gamma_p & \text{for} \quad TM-\text{modes} \end{cases} \tag{2}$$

where $y_0 = \sqrt{\varepsilon_0/\mu_0} = 1/(120\pi)$ mhos is the free space wave admittance, $y = y_0\sqrt{\varepsilon_r/\mu_r}$ and $k = \omega\sqrt{\varepsilon_0\varepsilon_r\mu_0\mu_r} = k_0\sqrt{\varepsilon_r\mu_r}$ is the wavenumber.

The eigenvalues of each mode (χ_{mn}, χ'_{mn}) are determined by imposing the boundary conditions at the waveguide wall ($\rho = a$) and are given as:

$$\begin{aligned} &J_m(\chi_{mn}) = 0 \text{ defines the } TM_{mn} \text{ eigenvalue } \chi_{mn} \\ &J'_m(\chi'_{mn}) = 0 \text{ defines the } TE_{mn} \text{ eigenvalue } \chi'_{mn} \end{aligned} \tag{3}$$

It is a common practice in the mode matching technique to employ the generalized scattering parameters since we aim at the analysis of complicated microwave networks. The generalized versus the ordinary (simple voltage ratios) scattering parameters are preferable because they are normalized with respect to the wave impedance which is different for each mode. This is also the reason why the mode functions in equation (1) are normalized with respect to the wave admittance. In this manner the generalized scattering parameters for each mode can be expressed as a function of the modal coefficients [10, p.16] as:

$$\begin{bmatrix} \mathbf{B}_p \\ \mathbf{F}_q \end{bmatrix} = \begin{bmatrix} \mathbf{S}_{11} & \mathbf{S}_{12} \\ \mathbf{S}_{21} & \mathbf{S}_{22} \end{bmatrix} \begin{bmatrix} \mathbf{F}_p \\ \mathbf{B}_q \end{bmatrix} \tag{4}$$

Thus, (F_p, B_q) and (F_q, B_p) are respectively the amplitudes of the inward and outward

waves at the junction as shown in figure 1. Moreover, in order for the field expressions to be independent from the magnitude of the excitation the mode functions are normalized to the mode propagating power at the junction (z=0). Namely, the Poynting vector is formed from the expressions given by Collin [8, p.357] and integrated over the waveguide own cross section to evaluate the propagation power.

$$P_p^{TE} = \sqrt{\frac{2e_{0m}}{\pi}} \frac{1}{\sqrt{\left(\chi'^2_{mn} - m^2\right) J_m\left(\chi'_{mn}\right)}} \tag{5a}$$

$$P_p^{TM} = \sqrt{\frac{2e_{0m}}{\pi}} \frac{1}{\chi_{mn} J'_m\left(\chi_{mn}\right)} \tag{5b}$$

where $$e_{0m} = \begin{cases} 1 & m \neq 0 \\ 2 & m = 0 \end{cases}$$

After the normalization the transverse mode functions are expressed as:

$$\bar{\mathbf{e}}_p(\rho,\varphi) = \begin{cases} P_p^{TE}\left[\hat{\rho}\frac{m}{\rho} J_m\left(\frac{\chi'_{mn}}{a}\rho\right)\sin(m\varphi) + \hat{\varphi}\frac{\chi'_{mn}}{a} J'_m\left(\frac{\chi'_{mn}}{a}\rho\right)\cos(m\varphi)\right] & \text{for TE-modes} \\ P_p^{TM}\left[-\hat{\rho}\frac{\chi_{mn}}{a} J'_m\left(\frac{\chi_{mn}}{a}\rho\right)\sin(m\varphi) + \hat{\varphi}\frac{m}{\rho} J_m\left(\frac{\chi_{mn}}{a}\rho\right)\cos(m\varphi)\right] & \text{for TM-modes} \end{cases} \tag{6a}$$

$$\bar{\mathbf{h}}_p(\rho,\varphi) = \begin{cases} P_p^{TE}\left[-\hat{\rho}\frac{\chi'_{mn}}{a} J'_m\left(\frac{\chi'_{mn}}{a}\rho\right)\cos(m\varphi) + \hat{\varphi}\frac{m}{\rho} J_m\left(\frac{\chi'_{mn}}{a}\rho\right)\sin(m\varphi)\right] & \text{for TE-modes} \\ P_p^{TM}\left[\hat{\rho}\frac{m}{\rho} J_m\left(\frac{\chi_{mn}}{a}\rho\right)\cos(m\varphi) + \hat{\varphi}\frac{\chi_{mn}}{a} J'_m\left(\frac{\chi_{mn}}{a}\rho\right)\sin(m\varphi)\right] & \text{for TM-modes} \end{cases} \tag{6b}$$

The above expressions are general and can be used to express the fields in both sides of the discontinuity. Also, all six components must be taken into account. Furthermore, there is coupling between TE and TM modes at the discontinuity. Namely, even with a TE incident wave, both TE and TM modes will be present in the reflected and transmitted fields. Thus, the boundary conditions at the discontinuity are imposed on the total electric and magnetic fields. The total fields result from the summation over the infinite set of excited modes. The boundary conditions at the discontinuity require the continuity for the transverse ($\bar{E}_t$, $\bar{H}_t$) field at the aperture (z=0, cross section of the small waveguide $\rho \le R_2$) and the vanishment of $\bar{E}_t$ at the conducting obstacle (z=0, $R_2 \le \rho \le R_1$). These are imposed as:

$$\sum_{p=1}^{\infty}\bar{\mathbf{e}}_p^{I}(\rho,\varphi)\left(\mathbf{Y}_p\right)^{-1/2}\left[\mathbf{F}_p+\mathbf{B}_p\right]=\begin{cases}0 & \text{for} \quad R_2\le\rho\le R_1\\ \sum_{q=1}^{\infty}\mathbf{e}_q^{II}(\rho,\varphi)\left(\mathbf{Y}_q\right)^{-1/2}\left[\mathbf{F}_q+\mathbf{B}_q\right] & \text{for} \quad \rho<R_2\end{cases} \tag{7a}$$

$$\sum_{p=1}^{M}\bar{\mathbf{h}}_p^{I}(\rho,\varphi)\left(\mathbf{Y}_p\right)^{1/2}\left[\mathbf{F}_p-\mathbf{B}_p\right]=\sum_{q=1}^{N}\bar{\mathbf{h}}_q^{II}(\rho,\varphi)\left(\mathbf{Y}_q\right)^{1/2}\left[\mathbf{F}_q-\mathbf{B}_q\right] \qquad \text{for} \quad \rho<R_2 \tag{7b}$$

Superscripts I and II denote the waveguide with the large radius (R_1) and the small one (R_2) respectively.

For computational reasons the infinite summations of equations (7) must be truncated to a finite number. It is also well understood that more modes should be taken into account for the waveguide with the large radius in order to achieve the same accuracy in both of them. It has been proved that the ratio of the number of modes M/N should be equal to the ratio of the waveguide radius R_1/R_2, [11], namely M/N=R_1/R_2 where M, N the number of modes assumed to be excited within the waveguides with radius R_1 and R_2.

The summation of equations (7) involves all the unknown modal coefficients F_p, B_p, F_q and B_q. In order to construct a system of equations with these unknowns, it is a common practice to inner multiply in turn equation (7a) by each of the electric field modal functions of the larger waveguide ($\bar{e}_j^{I}$), while for the magnetic field it is recommended to multiply equation (7b) by the small radius waveguide modal function ($\bar{h}_j^{II}$) [10, p.14]. This choice is justified by the fact that the boundary conditions for the transverse electric field ($\bar{E}_t$) applies on the whole cross-section of the larger waveguide as described above. Thus, in order to enforce $\bar{E}_t$ to be zero at the conducting part of the discontinuity we must inner multiply Eq. (7a) by the electric field modal functions of the larger waveguide ($\bar{e}_j^{I}$). In this manner, the contribution resulting from the conducting area ($R_2 \le \rho \le R_1$) is set to zero and the integration is then restricted over the aperture ($\rho \le R_2$). For the transverse magnetic field ($\bar{H}_t$) the boundary conditions require only its continuity at the aperture, while over the conducting area the unknown current densities are also involved. Thus, in order to restrict this condition over the aperture ($\rho \le R_2$) it is recommended to inner-multiply

Eq. (7b) by the magnetic field modal functions of the smaller waveguide ($\bar{h}_j^{II}$). In this manner mixed modal functions inner products are involved in the resulting equations. It is then:

$$\sum_{p=1}^{M} \int_{S_2} \bar{\mathbf{e}}_p^{I} \bar{\mathbf{e}}_j^{II} dS_2 \left(\mathbf{Y}_p\right)^{-1/2} \left[\mathbf{F}_p + \mathbf{B}_p\right] = \sum_{q=1}^{N} \int_{S_2} \bar{\mathbf{e}}_q^{II} \bar{\mathbf{e}}_j^{I} dS_2 \left(\mathbf{Y}_q\right)^{-1/2} \left[\mathbf{F}_q + \mathbf{B}_q\right] \quad \text{for} \quad j = 1,2,..,M \tag{8a}$$

$$\sum_{p=1}^{M} \int_{S_2} \bar{\mathbf{h}}_p^{I} \bar{\mathbf{h}}_j^{II} dS_2 \left(\mathbf{Y}_p\right)^{1/2} \left[\mathbf{F}_p - \mathbf{B}_p\right] = \sum_{q=1}^{N} \int_{S_2} \bar{\mathbf{h}}_q^{II} \bar{\mathbf{h}}_j^{II} dS_2 \left(\mathbf{Y}_q\right)^{1/2} \left[\mathbf{F}_q - \mathbf{B}_q\right] \quad \text{for} \quad j = 1,2,...,M \tag{8b}$$

The final separation of the unknowns is accomplished by integrating over the larger waveguide cross section (already done in Eq. (8) above) and using the mode orthogonality properties, e.g. [12]. In this manner all terms involving $\bar{e}_p^{I} \bar{e}_j^{I}$ with $p \neq j$ vanish, while the integrals of the terms $\bar{e}_p^{I} \bar{e}_j^{I}$ for p=j are equal to 2 (rather than the usual unity due to the normalization). Analogous results are obtained for the magnetic modal function integrals but using the two waveguides in vice-versa. Namely, the integrals of $\bar{h}_q^{II} \bar{h}_j^{II}$ vanish at $q \neq j$ and are equal to 2 for q=j. These manipulations yield the following system of equations in matrix form:

$$\left[\mathbf{F}_p + \mathbf{B}_p\right] = \left[\mathbf{Q}^e\right]_{qj} \left[\mathbf{F}_q + \mathbf{B}_q\right] \tag{9a}$$

$$\left[\mathbf{Q}^m\right]_{pj} \left[\mathbf{F}_p - \mathbf{B}_p\right] = \mathbf{F}_q - \mathbf{B}_q \tag{9b}$$

where:

$$\mathbf{Q}_{qj}^{e} = \frac{1}{2} \left(\mathbf{Y}_p\right)^{1/2} \left(\mathbf{Y}_q\right)^{-1/2} \int_{S_2} \bar{\mathbf{e}}_q^{II} \bar{\mathbf{e}}_j^{I} dS_2 \tag{10a}$$

$$\mathbf{Q}_{qj}^{m} = \frac{1}{2} \left(\mathbf{Y}_p\right)^{1/2} \left(\mathbf{Y}_q\right)^{-1/2} \int_{S_2} \bar{h}_p^{I} \bar{h}_j^{II} dS_2 \tag{10a}$$

The remaining coupling integrals of Q_{qj}^{e} and Q_{pj}^{m}, both of them over the small waveguide cross section (aperture S_2, $\rho < R_2$), must be evaluated either numerically or analytically. In fact only one of the two matrices of integrals, either $\left[Q^e\right]_{qj}$ or $\left[Q^m\right]_{pj}$ need to be evaluated because the one is equal to the transpose of the other. This results from the relation between electric and magnetic field modal functions, which in turn is referred to the relation between transverse ($\bar{E}_t$, $\bar{H}_t$) and longitudinal (E_z, H_z) field components coming directly from the two Maxwell rotational equations. It is simpler to see this from equation (6), which gives $\bar{h}_t(\rho,\varphi) = \hat{z} \times \bar{e}_t(\rho,\varphi)$.

Moreover, the modal functions $\bar{e}_q^{II}$, $\bar{e}_j^{I}$ and $\bar{h}_q^{II}$, $\bar{h}_j^{I}$ are different for TE and TM

modes as shown in equations (6a) and (6b). Thus, each one of equations (8a) and (8b) can be decomposed into four sets of equations which can be discriminated as TE-TE, TM-TM, TE-TM and TM-TE couplings. Each one of these combinations results into a different coupling integral.

Since these integrals include Bessel functions with different orders and different arguments they require an increased computational effort, especially for microwave network synthesis applications. Thus, their analytical evaluation is of primary importance. It is toward this aim that the present work tries to contribute.

Examining carefully the work of Wade and MacPhie [3], it can be realized that the transformation of cylindrical to rectangular coordinates ($A_x = A_\rho \cos(\varphi) - A_\varphi \sin(\varphi)$, $A_y = A_\rho \sin(\varphi) + A_\varphi \cos(\varphi)$) reduce the coupling integrals into a form with known analytical solutions. This is given by Abramowitz and Stegun [5, p.484] as:

$$\int_0^a J_m(x_1 r) J_m(x_2 r) r dr = \frac{a}{x_1^2 - x_2^2}\left\{x_1 J_{m+1}(x_1 a) J_m(x_2 a) - x_2 J_m(x_1 a) J_{m+1}(x_2 a)\right\} \quad (11)$$

Carrying out the transformation from cylindrical to rectangular coordinates, the modal functions take the form:

$$\bar{\mathbf{e}}_p(\rho,\varphi) = \begin{cases} P_p^{TE} \dfrac{\chi'_{mn}}{2R_1}\left\{\hat{x}\left[J_{m+1}\left(\dfrac{\chi'_{mn}}{R_1}\rho\right)S_+ + J_{m-1}\left(\dfrac{\chi'_{mn}}{R_1}\rho\right)S_-\right] + \hat{y}\left[-J_{m+1}\left(\dfrac{\chi'_{mn}}{R_1}\rho\right)C_+ + J_{m-1}\left(\dfrac{\chi'_{mn}}{R_1}\rho\right)C_-\right]\right\} & \text{TE-modes} \\ P_p^{TM} \dfrac{\chi_{mn}}{2R_1}\left\{\hat{x}\left[J_{m+1}\left(\dfrac{\chi_{mn}}{R_1}\rho\right)S_+ - J_{m-1}\left(\dfrac{\chi_{mn}}{R_1}\rho\right)S_-\right] - \hat{y}\left[J_{m+1}\left(\dfrac{\chi_{mn}}{R_1}\rho\right)C_+ + J_{m-1}\left(\dfrac{\chi_{mn}}{R_1}\rho\right)C_-\right]\right\} & \text{TM-modes} \end{cases}$$

(12)

where, $s_\pm = \sin[(m \pm 1)\varphi]$, $c_\pm = \cos[(m \pm 1)\varphi]$ and again $\bar{h}_t(\rho,\varphi) = \hat{z} \times \bar{e}_t(\rho,\varphi)$.

This form applies to both waveguides. Using the formulae given in equation (10) the four coupling integrals for the electric field are expressed as:

$$Q_{pq} = Q_{mn,il} = \begin{cases} P_p^{TE} P_q^{TE} \sqrt{\dfrac{\gamma_p}{\gamma_q}} \dfrac{\chi'_{mn}\chi'_{il}}{R_1 R_2}\left\{\Phi_{m+1} + \Phi_{m-1}\right\} & \text{for TE-TE coupling} \\ -P_p^{TE} P_q^{TM} \dfrac{\sqrt{\gamma_p \gamma_q}}{k_0} \dfrac{\chi'_{mn}\chi_{il}}{R_1 R_2}\left\{\Phi_{m+1} - \Phi_{m-1}\right\} & \text{for TE-TM coupling} \\ 0 & \text{for TM-TE coupling} \\ P_p^{TM} P_q^{TM} \sqrt{\dfrac{\gamma_q}{\gamma_p}} \dfrac{\chi_{mn}\chi_{il}}{R_1 R_2}\left\{\Phi_{m+1} + \Phi_{m-1}\right\} & \text{for TM-TM coupling} \end{cases} \quad (13)$$

where,
$$\Phi_k = \frac{R_2}{\left(\frac{\chi_{mn}}{R_1}\right)^2 - \left(\frac{\chi_{il}}{R_2}\right)^2}\left[\frac{\chi_{il}}{R_2} J_{k+1}\left(\frac{\chi_{mn}}{R_1} R_2\right) J_k(\chi_{il}) - \frac{\chi_{mn}}{R_1} J_{k+1}(\chi_{il}) J_k\left(\frac{\chi_{mn}}{R_1} R_2\right)\right]$$

while for the magnetic field is:

$$\left[\mathbf{Q}^{m}_{pq}\right] = \left[\mathbf{Q}^{e}_{pq}\right]^{T} \tag{14}$$

Using the above closed form expressions the coupling integrals can be evaluated very fast and they are in turn substituted into equations (9a) and (9b). This is a system of equations with totally (N+M) unknowns, namely M unknown reflected B_p;, p=1,2,..,M and N transmitted F_q;, q=1,2,..,N modal amplitudes. Since, we are actually interested in the generalized scattering parameters, the expressions for $\left[Q^{e}_{pq}\right]$ and $\left[Q^{m}_{pq}\right]$ are in turn substituted in equation (4) resulting in the final desired formulas as:

$$\begin{aligned}
\left[\mathbf{S}_{11}\right]_{pq} &= \left([\mathbf{Q}]_{pq}[\mathbf{Q}]^{T}_{pq} + [\mathbf{I}]\right)^{-1}\left([\mathbf{Q}]_{pq}[\mathbf{Q}]^{T}_{pq} - [\mathbf{I}]\right) \\
\left[\mathbf{S}_{12}\right]_{pq} &= 2\left([\mathbf{Q}]_{pq}[\mathbf{Q}]^{T}_{pq} + [\mathbf{I}]\right)^{-1}[\mathbf{Q}]_{pq} \\
\left[\mathbf{S}_{21}\right]_{pq} &= [\mathbf{Q}]^{T}_{pq}\left([\mathbf{I}] - \left[\mathbf{S}_{11}\right]_{pq}\right) \\
\left[\mathbf{S}_{22}\right]_{pq} &= [\mathbf{I}] - [\mathbf{Q}]^{T}_{pq}\left[\mathbf{S}_{12}\right]_{pq}
\end{aligned} \tag{15}$$

where $\left[\mathbf{Q}^{e}_{pq}\right] = \left[\mathbf{Q}_{pq}\right]$ and $\left[\mathbf{Q}^{m}_{pq}\right] = \left[\mathbf{Q}_{pq}\right]^{T}$

A lot of practical microwave structures can be decomposed into a series of waveguide discontinuities, (like the one shown in figure 1), connected in tandem. In this structure the output from one junction coincides with the input of the successive one. The input of the first junction is the excitation of the structure and can be any one or a combination of the input waveguide modes. The incident field at the output of the last junction depends on the terminating load, and it is evaluated accordingly, e.g. from the load reflection. Each waveguide can be assumed to be empty (filled with air) or to be homogeneously fulfilled with an isotropic dielectric or magnetic material. The material properties are also included in the above formulation in order to allow the analysis of filters or any structure including for example dielectric windows, e.g. [14]. Moreover, structures like cylindrical corrugated horns can be equally well analyzed.

In order to verify the analytical part of the above formulation a dominant mode (TE_{11}) incident field is first considered. For this case the coupling integrals of equation (10) are already given by Wu [2, p. 277] in closed form. In this case the present

method expressions given in equation (13) are exactly reduced to those of [2].

3. NUMERICAL RESULTS

Our primary aim was to develop a fast mode matching technique which should be able to handle complicated cylindrical waveguide structures. A lot of structures have been analyzed in order to verify this aim and some characteristic examples are given bellow.

One of our first concerns was the numerical verification of the present formulation. For this purpose a thick cylindrical iris, shown in figure 2a, has been analyzed for different diameters and thicknesses. The results for the magnitude and phase of the S_{11} parameter are shown in figure 2b, where its thickness is varied (t=0.1 to 100mm) and its diameter (2b) is kept constant (b=9.525mm). These results are in a very good agreement with those of a moment method solution (MoM) [13] as well as with the corresponding measurements [13]. This investigation was repeated for various diameters, where our results are always almost identical to those of the MoM solution, while the maximum deviation from measurements was of the order of 1% for the magnitude and phase. A similar investigation for a constant iris thickness t=5.08mm and varying its diameter is shown in figure 2c.

An iris matched dielectric window shown in figure 3a, is analyzed in [14] using a «recurrence modal analysis» and considering a dominant mode excitation. This structure has been optimized in [14] for f/f_c=1.1. The present results for the reflection $|S_{11}|$ and transmission $|S_{21}|$ coefficients magnitudes are compared against those of [14], (only $|S_{11}|$ is available in [14]), as shown in figure 3b and found to be almost identical.

In order to show the validity of the present formulation for excitation other than the dominant, the computer optimized filter (figure 4a) is analyzed for a TE_{01} excitation. The results for the insertion loss is shown in figure 4b and compared with those given therein. An excellent agreement is observed.

Our next concern was to prove the efficiency of the proposed method regarding its speed and its ability to handle complicated structures. For this purpose the corrugated horn antenna proposed in [16] was analyzed. This antenna has a semi-flare angle of 4 degrees and aperture radius of 3.14cm and is decomposed into 1235 cylindrical waveguide sections, which in turn constitute 1234 waveguide discontinuities. Dragone, employed an approximate method for the analysis of corrugated horns and

also provided us with measurements for the $|S_{11}|$.

This corrugated horn was analyzed herein by employing both the present formulation as well as the commercial package of TICRA [6]. The results for the $|S_{11}|$ are shown in figure 5. The present method gives identical results with those of TICRA, but at a small fraction of CPU time as one can see from figure 6. Both methods give a good convergence with 35 modes. A satisfactory agreement between the present method and the measurements is observed. Especially, for frequencies above 32GHz our method performs quite better than that of [16].

Moreover, the present method is quite faster than that of TICRA as shown in figure 6, where the required CPU time is plotted against the number of modes at the aperture. At least 15 modes are required for the method to start converging, while about 35 modes are required for accurate results. Both programs are executed on a PC-486. Taking into account that in the usual practice the analysis method should be included within a CAD package for the design of such structures, the present method is obviously preferable. The results for the H- and E- plane radiated field are shown in figure 7, for a frequency of 23, 29 and 35GHz. The far field is calculated by first evaluating the electric field at the aperture (or the equivalent magnetic current density) which is in turn integrated over the aperture to obtain the far field [7]. It must be noted that the latter is an approximate method, since the discontinuity between the aperture and the free space as well as the outer conducting part of the antenna, are not taken into account. Finally it can be easily deduced from the examples studied above that the proposed method is ready to be included in microwave network synthesis algorithms and this is actually our next goal.

a)

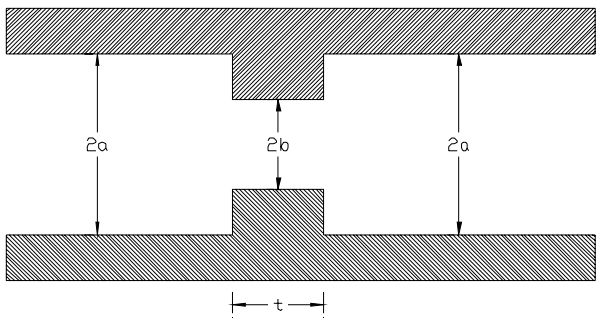

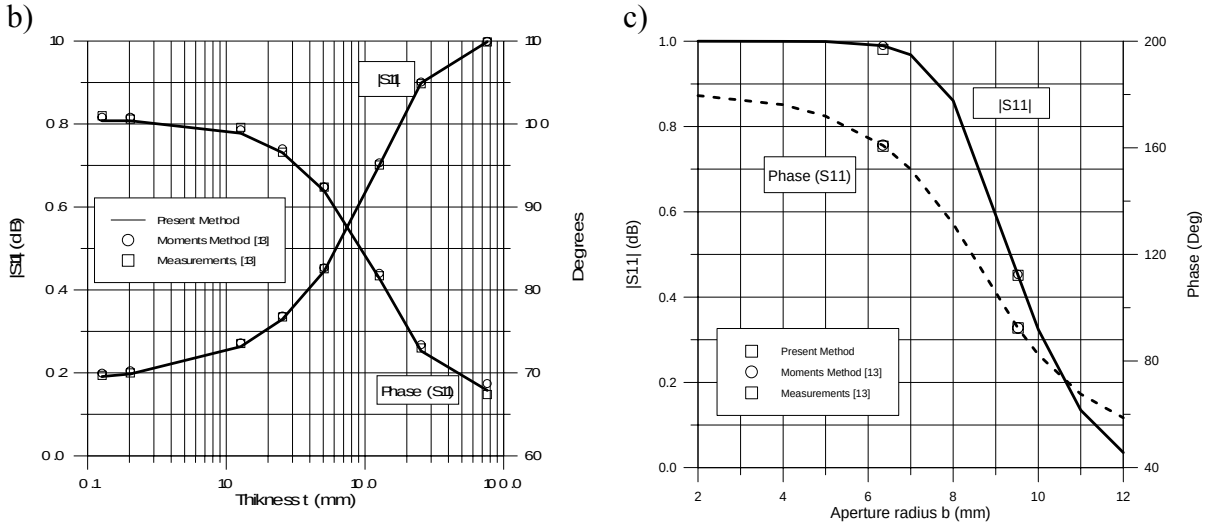

Figure 2. Reflection and transmission coefficient of an iris, varying the iris thickness (t) and diameter (b), (f=9 GHz, a=12.74445mm), a) geometry of a thick iris., b) varying the iris thickness for fixed diameter b=6.35mm, c) varying the iris diameter for a fixed thickness t=10.0mm.

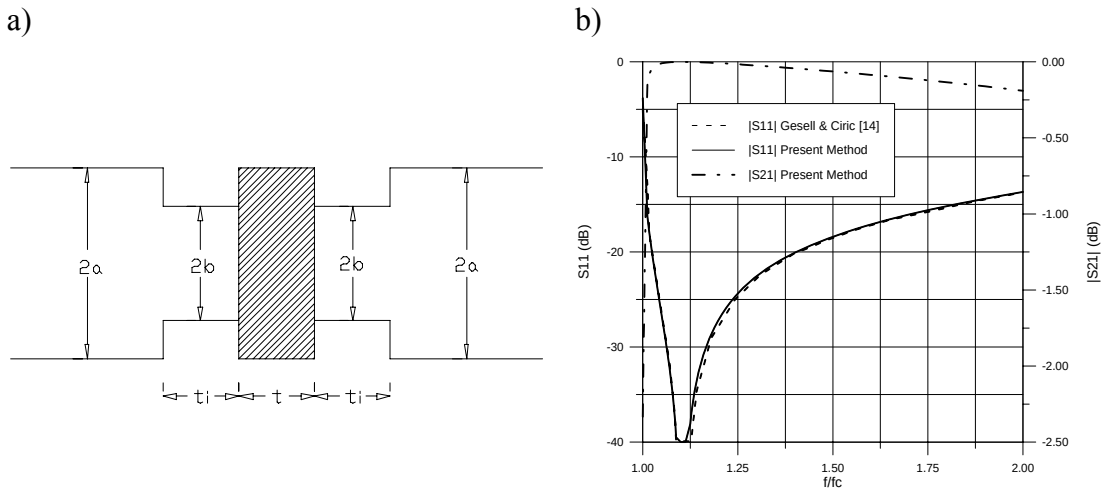

Figure 3. An iris matched dielectric window [14] with f / f_c=1.1, ε_r=2.8, t/a=0.04 and t_i=t, a=10.0mm, b=8.63mm, f_c=8.79GHz, a) geometry of the iris, and b) results for $|S_{11}|$ and $|S_{21}|$.

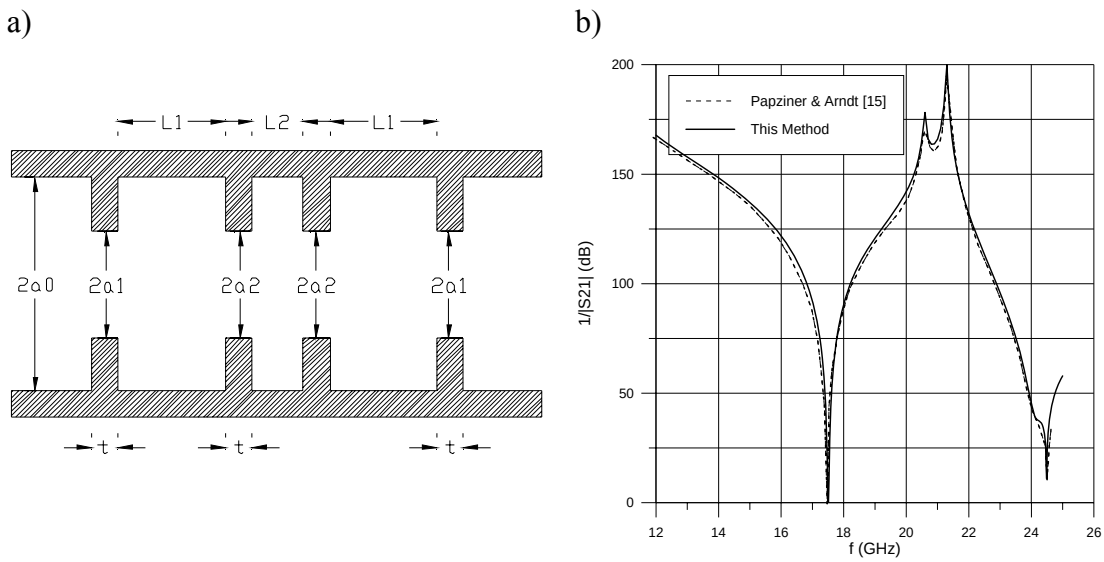

Figure 4. A TE_{01} excited mode filter [15]. (a0=16.269mm, a1=6.718mm, a2=3.888mm, l1=11.142mm, l2=10.907mm, t=0.2mm), a) geometry of the filter, and b) results for the insertion loss.

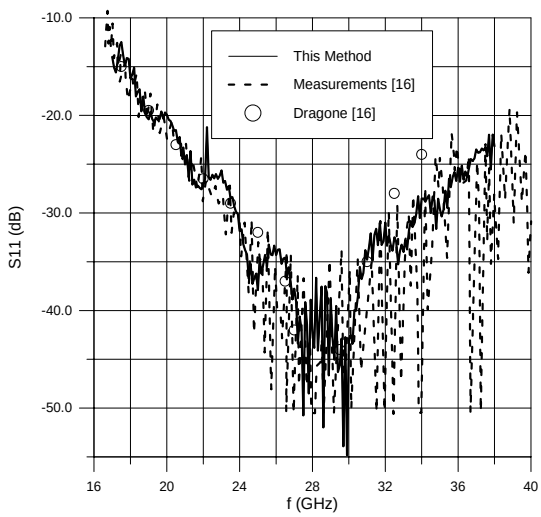

Figure 5. Results for the return loss of a corrugated horn proposed in [16].

4. CONCLUSIONS

A fast and accurate mode matching technique for the analysis of cylindrical structures that can be decomposed into multiple concentric step discontinuities, is proposed. The coupling integrals involved are evaluated analytically and the resulting closed form expressions are theoretically verified for the special case of a dominant mode excitation. For different excitations as well as for a number of applications the results are in a very good agreement with measurements and/or results given by other methods. The technique proposed herein is appropriate to be included in microwave network synthesis algorithms.

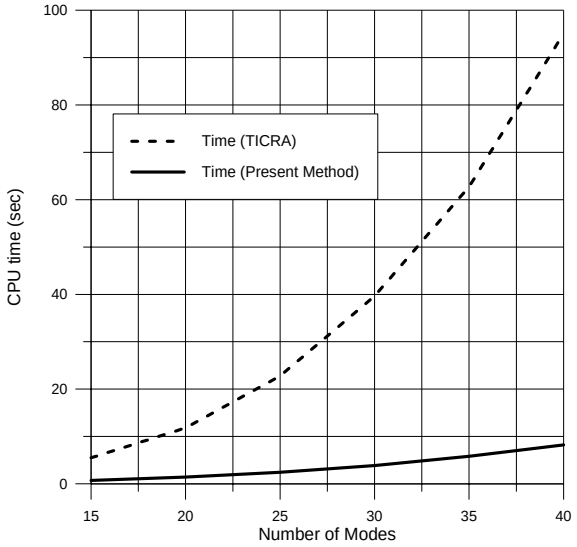

Figure 6. Required CPU time for the analysis of the corrugated horn proposed in [16].

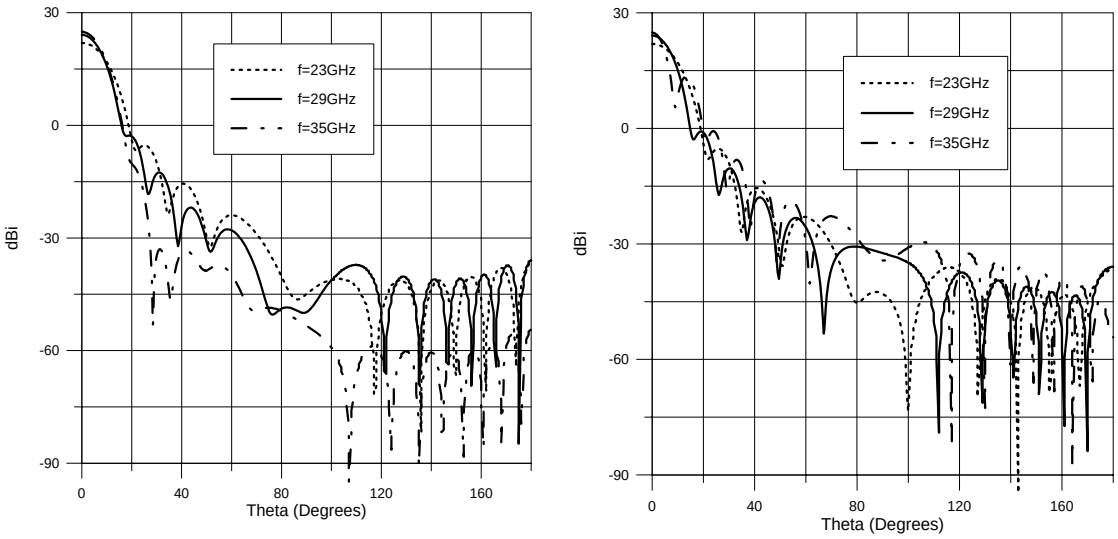

Figure 7. H- and E- plane radiation patterns of a corrugated horn [16].

REFERENCES

[1] E. Alessandri, M. Dionigi and R. Sorrentino, «A Fullwave CAD tool for waveguide components using a high speed direct optimizer», IEEE Trans. on Microwave Theory and Techniques, vol. MTT-43, pp. 2046-2052, September 1995.

[2] C.P. Wu, «Variational and iterative methods for waveguides and arrays», in R. Mittra, (Editor) «Computer techniques for Electromagnetics», Summa Book, 2nd Edition, 1987.

[3] J.D.Wade, and R.H. MacPhie, «Scattering at circular to rectangular waveguide junction», IEEE Trans. on Microwave Theory and Techniques, vol. MTT-

34,.1085-1091,November 1986

[4] R.H. MacPhie, and K.L. Wu, «Scattering at the junction of a rectangular waveguide and a larger circular waveguide», IEEE Trans. on Microwave Theory and Techniques, vol. MTT-43, pp.2041-2045, September 1995

[5] M. Abramowitz and I.A. Stegun, «Handbook of mathematical functions», Dover, New York, 1965.

[6] CHAMP: «Conical Horn Analysis by Modal Processing», @ TICRA, Copenhagen 1990

[7] R.E. Collin and F.J. Zucker, «Antenna Theory», McGraw Hill, 1969.

[8] R.E. Collin, «Field theory of guided waves», IEEE Press, 1991.

[9] T.S. Bird, «Analysis of mutual coupling in finite arrays of different-sized rectangular waveguides», IEEE, Trans. on Antennas and Propagation, vol. AP-38, no. 2, pp. 166-172, February 1990.

[10] J. Uher, J. Bornemann and U. Rosenberg, «Waveguide components for antenna feed systems: Theory and CAD», Artech House, 1993

[11] P.H. Masterman and P.J.B. Clarricoats, «Computer field-matching solution of waveguide transverse discontinuities», IEE Proc., vol. 118, no. 1, pp. 51-63, January 1971.

[12] A. Wexler, «Solution of waveguide discontinuities by the modal analysis», IEEE Trans. on Microwave Theory and Techniques, vol. MTT-15, no. 9, pp. 508-517, September 1967.

[13] R.W. Sharstein and A.T. Adams, «Thick circular iris in a TE_{11} mode circular waveguide», IEEE Trans. on Microwave Theory and Techniques, vol. MTT-36, no.11, pp.1529-1531, November1988.

[14] G. Gesell and I.R. Ciric, «Recurrence modal analysis for multiple waveguide discontinuities and its application to circular structures», IEEE Trans. on Microwave Theory and Techniques, vol. MTT-41, no. 3, pp.484-490, March 1993.

[15] U.Papziner and F. Arndt, «Field theoretical computer aided design of rectangular and circular iris coupled rectangular or circular waveguide cavity filters», IEEE Trans. On Microwave Theory and Techniques, vol. MTT-41, no. 3, pp.462-471, March 1993.

[16] C. Dragone, «Reflection, transmission and mode conversion in a corrugated feed», Bell Syst. Tech. J., vol. 56, no. 6, pp. 835-867, 1977.